Chapter: 2

Synthesis of Phase Pure BMT-PT and BMZ-PT

Chapter-2

2.1 Introduction

As discussed in previous chapter, $Bi(Mg_{1/2}Ti_{1/2})O_3$ [BMT] cannot be synthesized in pure perovskite form at ambient pressure using traditional solid state ceramics method due to lower tolerance factor. Pure perovskite phase of $Bi(Mg_{1/2}Ti_{1/2})O_3$ can be synthesized only by calcining the reactant mixture at high temperature (1270K) under high pressure (6GPa). For the preparation of phase pure $Bi(Mg_{1/2}Ti_{1/2})O_3$, high temperature (1270K) and high pressure (6GPa) is required because $Bi(Mg_{1/2}Ti_{1/2})O_3$ is a metastable perovskite [Khalyavin et al. (2006); Yoneda et al. (2011)]. The high pressure technique restricts the magnitude of tolerance factor $0.75<t<1.06$ in perovskite ABO_3 type structure. The perovskite structure favours the less closed packed structure which can be stabilized in case of $Bi(Mg_{1/2}Ti_{1/2})O_3$ under pressure easily. The solid solution formation of $Bi(Mg_{1/2}Ti_{1/2})O_3$ with other stable ABO_3 type perovskites can also be used to synthesize phase pure material at ambient pressure synthesis. Formation of solid solution of $Bi(Mg_{1/2}Ti_{1/2})O_3$ with other ABO_3 type of perovskites not only helps to reduce the formation of non-perovskite impurity phases but also enhances the piezoelectric properties and the planar electromechanical coupling coefficients. Solid solution formation of $Bi(Mg_{1/2}Ti_{1/2})O_3$ with $PbTiO_3$, $PbZrO_3$, and $BaTiO_3$ stabilizes perovskite phase for synthesis at ambient pressure. Similarly to BMT, the synthesis of phase pure perovskite structure of $Bi(Mg_{1/2}Zr_{1/2})O_3$ [BMZ] at ambient temperature and pressure is also not possible. BMZ can also be stabilized in perovskite structure

at ambient pressure by the formation of its solid solution with other stable perovskites. In present work we have stabilised BMT and BMZ by forming its solid solution with $PbTiO_3$.

In this chapter, the experimental details for synthesis of phase pure (1-x)$Bi(Mg_{1/2}Ti_{1/2})O_3$-x$PbTiO_3$ and (1-x)$Bi(Mg_{1/2}Zr_{1/2})O_3$-x$PbTiO_3$ solid solutions are given for the composition range, $0.25 \leq x \leq 0.45$ and $0.55 \leq x \leq 0.61$ respectively, by using conventional solid state ceramic route. It is shown that the formation of impurity phases commonly observed during the synthesis of pure $Bi(Mg_{1/2}Ti_{1/2})O_3$ and $Bi(Mg_{1/2}Zr_{1/2})O_3$ can be completely suppressed by the formation of solid solution with PT. Before we present the details of synthesis and sample characterization, a brief overview of characterization techniques used in this work are presented below.

2.2 Characterization tools

2.2.1 X- ray diffraction

X-ray diffraction (XRD) is used to characterize, determine and identify the phase purity and structure of pellets and powders sample. Powders Sample mounted in a glass plate is loaded into the diffractometer for data collection. Phase identification can also be done by matching the XRD pattern of the materials with reference patterns from JCPDS–ICDD files. Diffraction occurs, when any electromagnetic radiation interacts with a periodic structure. X-rays have wavelengths of the order of a few angstroms which is typical inter-atomic distance in crystalline solids. When X-rays are scattered from a crystalline solid, they can constructively interfere, producing a diffracted beam. X-ray diffraction

(XRD) measurements were carried out using an 18kW rotating anode (CuKα) based Rigaku (RINT 2000/PC series) powder diffractometer operating in the Bragg-Brentano geometry and fitted with a curved crystal graphite monochromator in the diffracted beam. The measurements were done at scan speed of 2 degrees/min using scan step 0.02 degree.

Bragg's law:

Sir William H. Bragg and Sir W. Lawrence Bragg have given a relationship, describing the angle at which a beam of X-rays of a particular wavelength diffracts from a crystalline surface known as Bragg's Law.

$$2d \sin\theta = n\lambda \qquad (2.1)$$

λ = wavelength of the x-ray

θ = scattering angle

n = integer, represents the order of the diffraction peak

d = inter planer distance of (i.e atoms, ions, molecules)

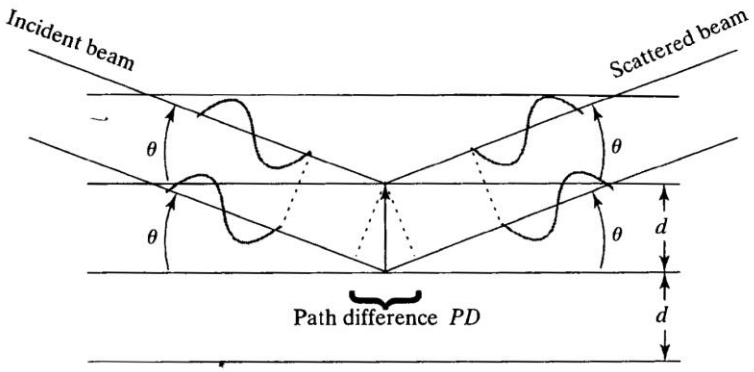

Fig.2.1 Schematic diagram of X-ray diffraction.

The X-ray diffraction pattern of a given powder sample is obtained by measuring the scattered intensity with the variation of the angle (2θ). Quantitative information on single phase and multi-phase materials can also be obtained using pattern calculation by full diffraction pattern fitting methods (Rietveld refinement). This approach can give accurate values for sample composition, crystal symmetry, unit-cell dimensions, atom positions, site-occupancy factors and many more for pure as well as doped samples.

2.2.2 Scanning Electron Microscope (SEM) and Energy Dispersive X-ray analysis (EDS)

Accelerated electrons carry significant amount of kinetic energy (KE), which is dissipated in variety of signals produced by "electron-sample interactions" when the incident electrons are decelerated by the sample. In an optical microscope, magnification is obtained by a system of 'optical lenses'. The smaller is the wavelength of light, the greater is its resolving power which sets a limit over the optical microscope. In electron microscope, wavelength of the radiation can be decreased significantly by changing the accelerating voltage of electron and thereby momentum of the electron matter wave. That is why, despite its smaller numerical aperture, an electron microscope can resolve objects as small as 0.001μ (=10Å), as compared to 0.2μ by a light microscope. Thus, the resolving power of an electron microscope is 200 times greater than that of a light microscope. SEM analysis is considered to be "non-destructive" as the x-rays generated by electron sample interactions do not lead to volume loss of the sample. Thus it is possible to analyse the same materials repeatedly.

The microstructure of the investigated sample was characterized using a field emission gun based scanning electron microscope (SEM) (Supra 40, Zeiss, Germany), equipped with energy dispersive x-ray analyser. Before recording SEM images, the surface of sintered pellets were coated with conducting gold film by sputtering under vacuum. Electron Source (Gun) voltage was varied during the SEM analysis to produce better contrast in the images. Energy dispersive x-ray spectroscopy (EDS) is used for compositional analysis available with mentioned SEM. Its characterization principle is that each element has a unique electronic energy state which is the characteristic of that element. So the characteristic x-rays emitted by different elements in the sample are distinguishable from one another due to difference in x-ray photon energy.

2.3 Experimental details

The solid state ceramic route is the most widely used technique for the synthesis of polycrystalline solids from starting materials. A thermochemical reaction in homogeneous mixture of reactant powders at high temperature results to product powder. The feasibility and rate of a solid state reaction depends on reaction conditions, calcination temperature, structural properties of the reactants, and surface area of the solids, their reactivity and the thermodynamic free energy change associated with the reaction.

In this section we provide the details of the experimental procedures for the synthesis of $(1-x)Bi(Mg_{1/2}Ti_{1/2})O_3$-$xPbTiO_3$ and $(1-x)Bi(Mg_{1/2}Zr_{1/2})O_3$-$xPbTiO_3$. The conventional solid state ceramic route/method was used for the synthesis of $(1-x)Bi(Mg_{1/2}Ti_{1/2})O_3$-$xPbTiO_3$ and $(1-x)Bi(Mg_{1/2}Zr_{1/2})O_3$-$xPbTiO_3$

in the composition range $0.25 \leq x \leq 0.45$ and $0.50 \leq x \leq 0.61$ respectively. For the preparation of samples we have used standard analytical reagent grade Bi_2O_3 (99.5%), TiO_2 (99%), PbO (98%), ZrO_2 (99.0%) and magnesium carbonate (light) with minimum MgO (40%). The reactant powders were characterized by x-ray diffraction before using them. The XRD patterns of Bi_2O_3, TiO_2, ZrO_2, PbO, and MgO are shown in Fig. 2.2. The observed diffraction patterns were compared with the patterns in ICDD database. The XRD patterns of the reactant powders are in well agreement with the reported ICDD data base [Bi_2O_3, File No. 010709, TiO_2, File No. 894921, ZrO_2, File No. 780048, PbO, File No. 050561, and MgO, File No. 040829,].

2.3.1 Weighing and mixing

Initial raw materials were weighed in the stoichiometric ratio using analytical balance (CA-223) and thoroughly mixing in an agate mortar pestle for 1-2 hours. This mixture was ball Milled in a planetary ball mill (Retsch GmbH, Germany) for 6h using agate jars (500ml) and agate balls of 10mm diameter using analytical reagent grade acetone as mixing medium. The ball-to-powder ratio was 2:1 by weight. The milling was carried out at 100rpm with the rotation of jars in both the clockwise and counter clockwise directions.

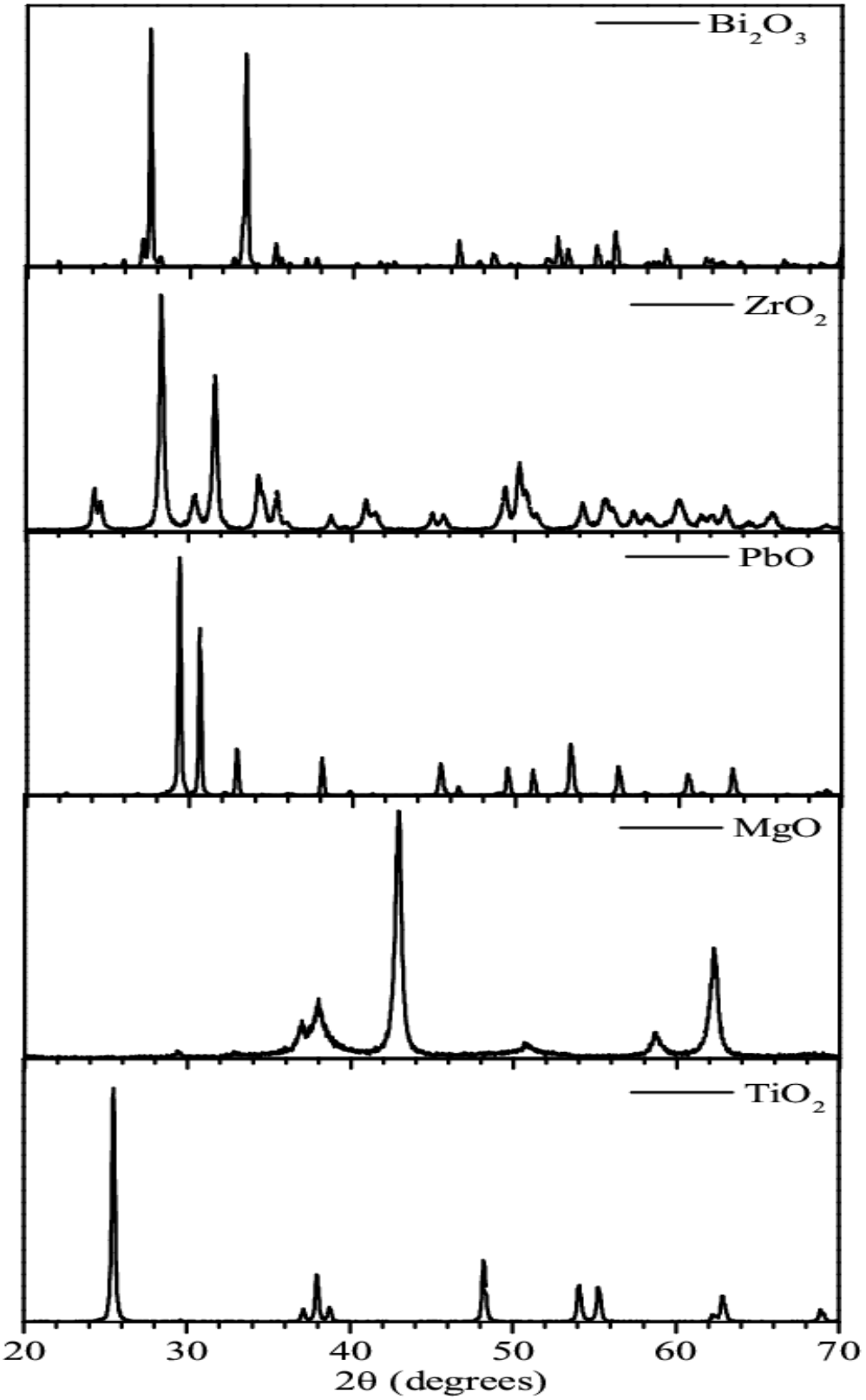

Fig.2.2 The XRD patterns of starting ingredients (a) Bi_2O_3, (b) ZrO_2, (c) PbO, (d) MgO and (d) TiO_2.

2.3.2 Calcination

The obtained ball milled power was dried in open air and kept in alumina crucibles and then calcined in a muffle furnace (capable of going up to ~1000^{o}C) at different temperatures 750^{o}C, 800^{o}C and 850^{o}C for 6h. The calcined powders were crushed into fine powders using agate mortar pestle. The x-ray diffraction pattern of the powders calcined at different temperatures is shown in Fig. 2.3. The peaks corresponding to perovskite phase are marked with letter 'P' in Fig. 2.3.

As can be seen in Fig. 2.3, perovskite phase starts forming at 750^{o}C. However, there are many impurity reflections. As we increase the calcination temperature, intensity of the peaks corresponding to impurity phases decreases gradually and dominant perovskite phase increases [Upadhyay et al. 2014]. Some impurity phases are still observed for the calcination temperature 800^{o}C, whose XRD peaks are marked by asterisk. Pure perovskite phase is obtained for the calcination temperature of 850^{o}C. In all these cases the calcination time was for 6h.

The calcination temperature was optimized similarly in case of BMZ-PT samples. The XRD patterns of BMZ-PT for the composition with x=0.55 calcined at 700^{o}C, 750^{o}C, and 775^{o}C for 6h is shown in Fig. 2.4. As can be seen from Fig. 2.4 the optimum calcination temperature for BMZ-PT piezoceramics is 775^{o}C, which gives nearly pure perovskite phase.

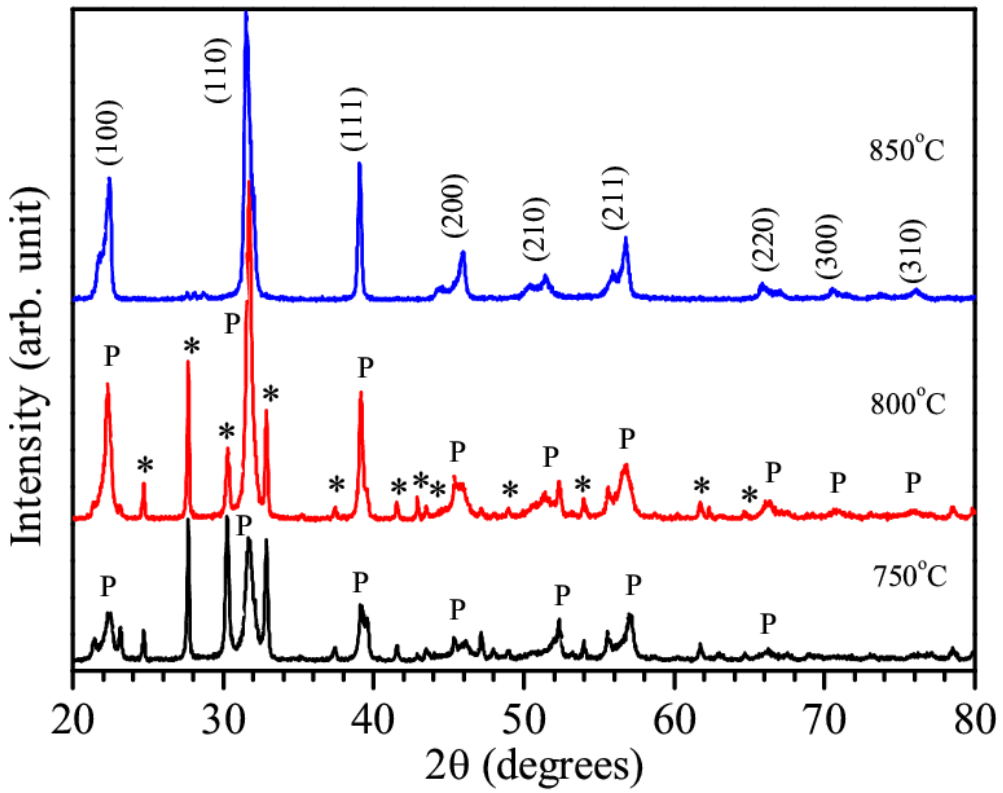

Fig.2.3 XRD profiles of BMT-PT ceramic with x=0.37 calcined at 750°C, 800°C and 850°C for 6h [Upadhyay et al. 2014].

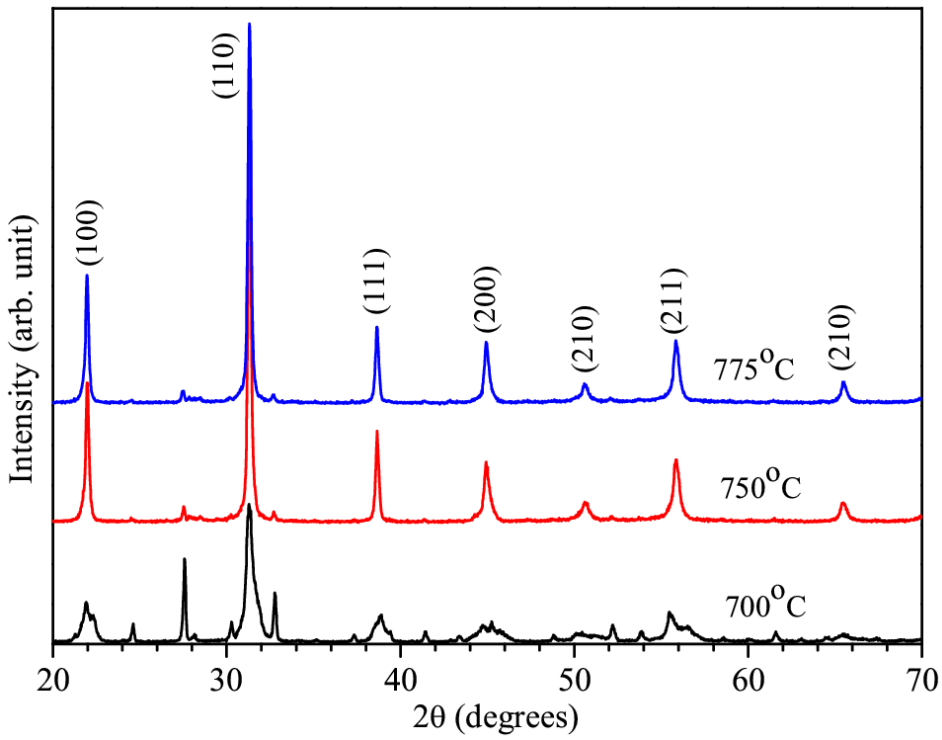

Fig.2.4 XRD patterns of 0.45BMZ-0.55PT piezoceramic calcined at 700°C, 750°C and 775°C for 6h.

2.3.3 Preparation of green pellets

After crushing, the calcined powers were mixed with a few drops of 2% polyvinyl alcohol (PVA) solution as binder, using an agate mortar pestle. Cold compaction of calcined powders was done in the form of circular pellets by using uniaxial hydraulic press and a steal die of 12mm diameter. The powder were put in the die and set in the hydraulic press. Then the die containing the powders is pressed. The obtained pellets are known as green pellets. The green density was measured for the pellets, prepared at different load. It was found that 65kN is the optimum load to get maximum green density. The green pellets were kept at 500^{o}C for 12h to burn off the binder (PVA) in a muffle furnace.

2.3.4 Sintering

Proper sintering of the green pellets is essential for obtaining high density and good electrical properties of the sample. Sintering of the samples were carried out in a sealed alumina crucible in a muffle furnace. Sacrificial amount of Bi_2O_3 and PbO powders were used as a spacer powder to prevent Bi_2O_3 and PbO loss from the pellets during sintering. The sealing was done by fired powder of MgO to avoid the loss of lead and bismuth oxide during high temperature sintering process. Sintering temperature and sintering period were properly optimized to get the maximum possible density. The optimum sintering temperature was found as 950^{o}C for BMT-PT and 975^{o}C for the BMZ-PT with the sintering duration of 3h. The percentage weight loss of PbO and Bi_2O_3 during sintering was found to be negligible.

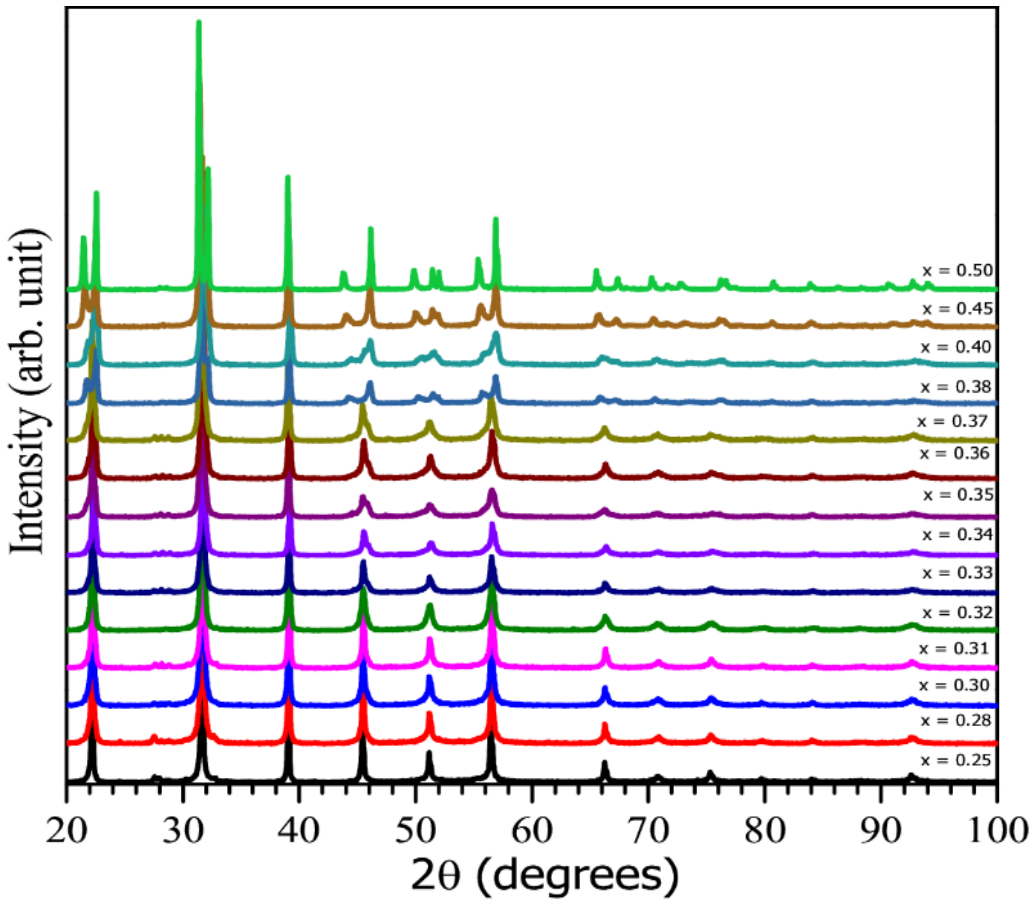

Fig.2.5 (a) XRD patterns of BMT-PT for different compositions sintered at 950^{o}C for 3h.

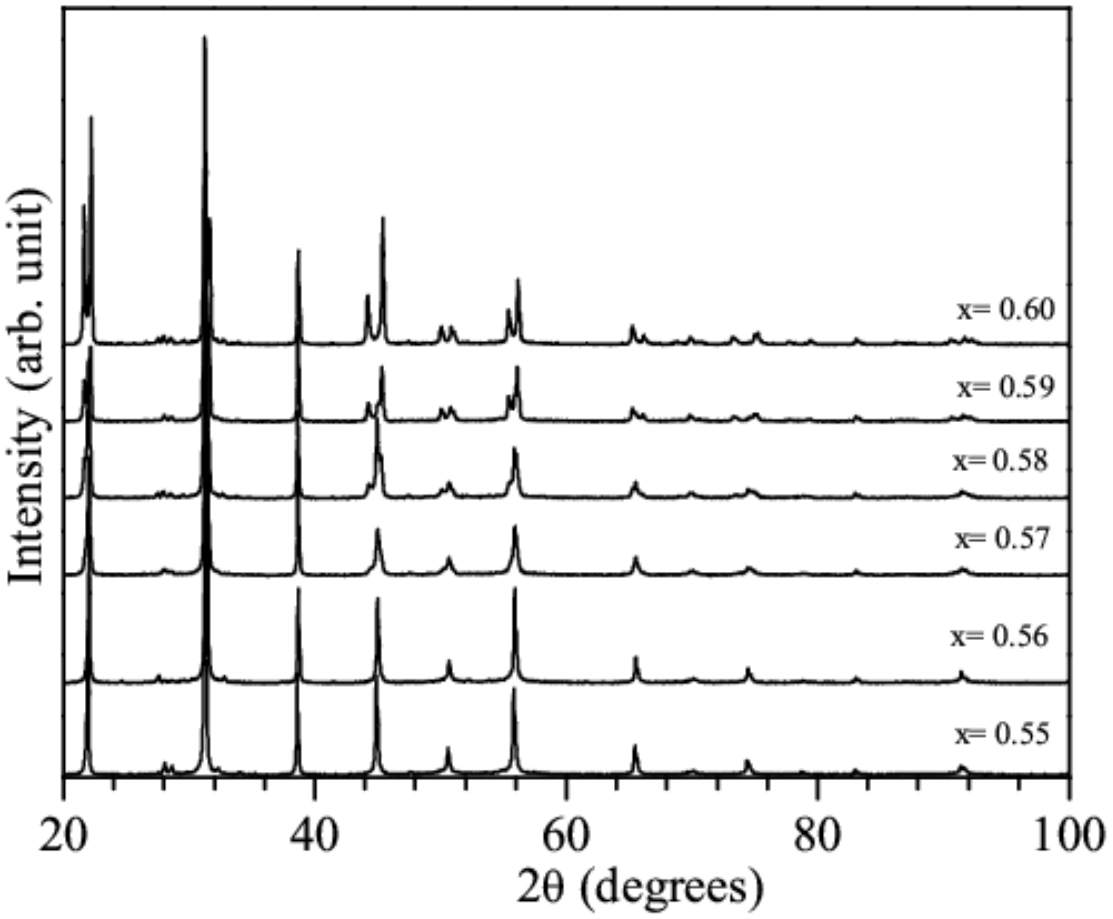

Fig.2.5 (b) XRD patterns of BMZ-PT for different compositions sintered at 975^{o}C for 3h.

The bulk density of the sintered pellets was calculated using liquid displacement method. It was found higher than 97% of the theoretical density for most of the sintered pellets. For x-ray characterizations, sintered pellets were crushed into fine powder and then annealed at 500^{o}C for 12h to remove the mechanical strains introduced during sintering and crushing. The XRD patterns of the sintered and annealed powders of BMT-PT and BMZ-PT at close compositional interval in the composition rage $0.25<x<0.45$ and $0.50<x<0.60$ are shown in Fig. 2.5 (a) and Fig. (b). All the peaks in the XRD patterns of the sintered powders could be indexed with the pure perovskite phase. Very small amount of impurity phase (less than 1%) is observed in BMZ-PT samples and lower composition of BMT-PT samples.

2.3.5 Microstructure and compositional studies

The scanning electron microscopic analysis of the sintered pellets was done to determine the grain size and uniformity of microstructure. EDS analysis was carried out to confirm the chemical compositions of the synthesized samples. Fig. 2.6 shows the SEM image of BMT-PT ceramics for the compositions with $x=0.40$, and BMZ-PT for the composition with $x=0.56$. SEM images show highly dense grain morphology. The average grain sizes was determined by linear intercept method, and found to be 0.5μm to 1μm and 1μm to 2 μm for BMT-PT and BMZ-PT piezoceramics respectively.

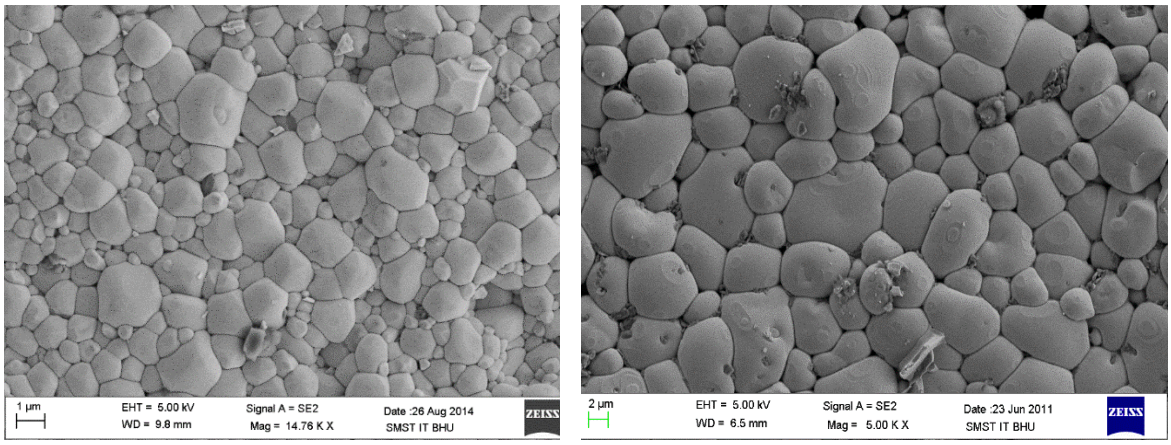

Fig.2.6 (a) SEM image of BMT-PT for composition x=0.40, and (b) SEM image of BMZ-PT for composition x=0.56.

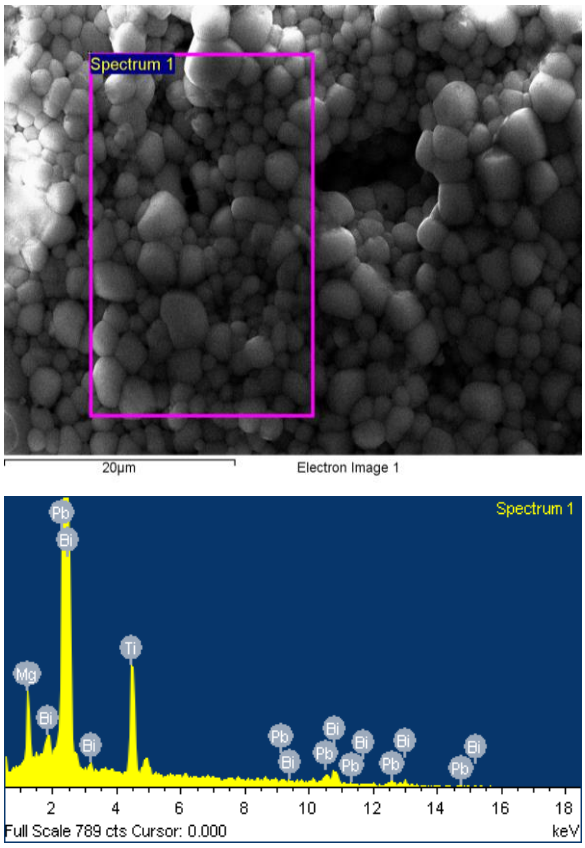

Fig.2.7 (a) SEM image and EDS spectrum of BMT-PT for the composition with x=0.35.

EDS spectra of BMT-PT and BMZ-PT ceramics are shown in Fig. 2.7 (a) and (b) for the compositions with x=0.35, and x=0.56 respectively. Since, the oxygen atom is very less sensitive to the x-ray diffraction due to low atomic scattering factor (Z=8), therefore the average atomic percentage of oxygen atom cannot be determined accurately from the EDS spectrum. This inaccuracy in atomic percent of oxygen atoms also disturbs the atomic percentages of other atoms. Therefore, in order to examine the composition (x) of the synthesized solid solutions more accurately, the EDS analysis was carried out for Bi, Pb, Mg, Zr and Ti only ignoring oxygen. The composition of the sample determined from EDS analysis are in well agreement with the nominal composition within the experimental error. The average atomic percentage observed for Pb, Bi, Mg and Ti atoms from EDS are given in Table 2.1 for 0.65BMT-0.35PT piezoceramics. The loss percentage during sintering in the atomic percentage is very small.

Table 2.1: Results of EDS analysis of atomic percentage for 0.65BMT-0.35PT ceramics, calcined at 850^{o}C and sintered at 950^{o}C.

Elements	**Atomic (%) (Calcined)**	**Atomic (%) (Sintered)**
Bi	32.35	32.71
Pb	15.37	15.14
Mg	18.33	20.27
Ti	33.95	31.88

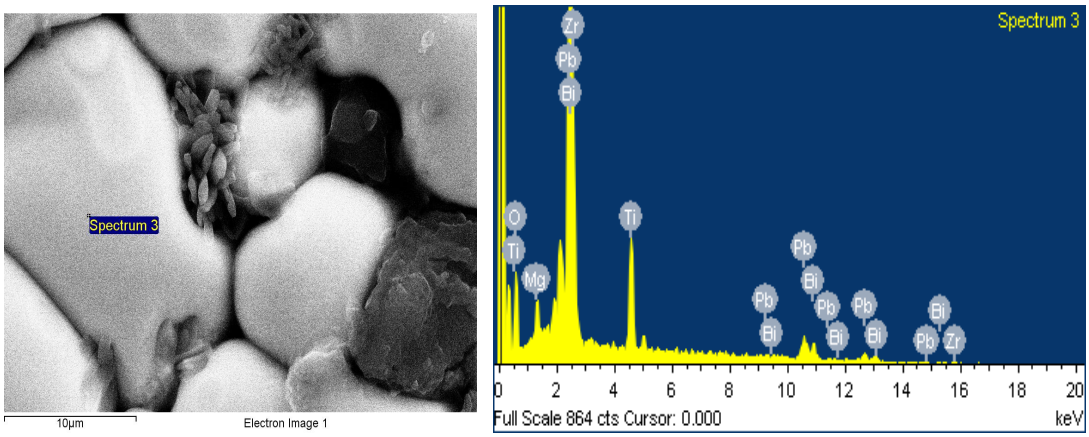

Fig.2.7 (b) SEM image and EDS spectrum of BMZ-PT for the composition with x=0.56.

2.4 Conclusions

Phase pure samples of (1-x)$Bi(Mg_{1/2}Ti_{1/2})O_3$-x$PbTiO_3$ and (1-x)$Bi(Mg_{1/2}Zr_{1/2})O_3$-x$PbTiO_3$ were synthesized under optimized conditions by conventional solid state ceramic route using Bi_2O_3, ZrO_2, MgO TiO_2 and PbO as initial ingredients. Substitution of $PbTiO_3$ has been found to be very effective in the reduction of intermediate impurity phases like $Bi_{12}TiO_{20}$ commonly formed during the synthesis of pure $Bi(Mg_{1/2}Ti_{1/2})O_3$ under ambient pressure. The average particle size of the calcined powders was 100nm to 300nm. The average grain size of the sintered samples prepared by this method are in the range of 0.5µm to 1.5µm. EDS analysis confirms that stoichiometric compositions were formed. In the next chapter we will present the result of structural characterization of these samples at room temperature.